

SUPPLEMENTARY INFORMATION

SUPPLEMENTARY FIGURES

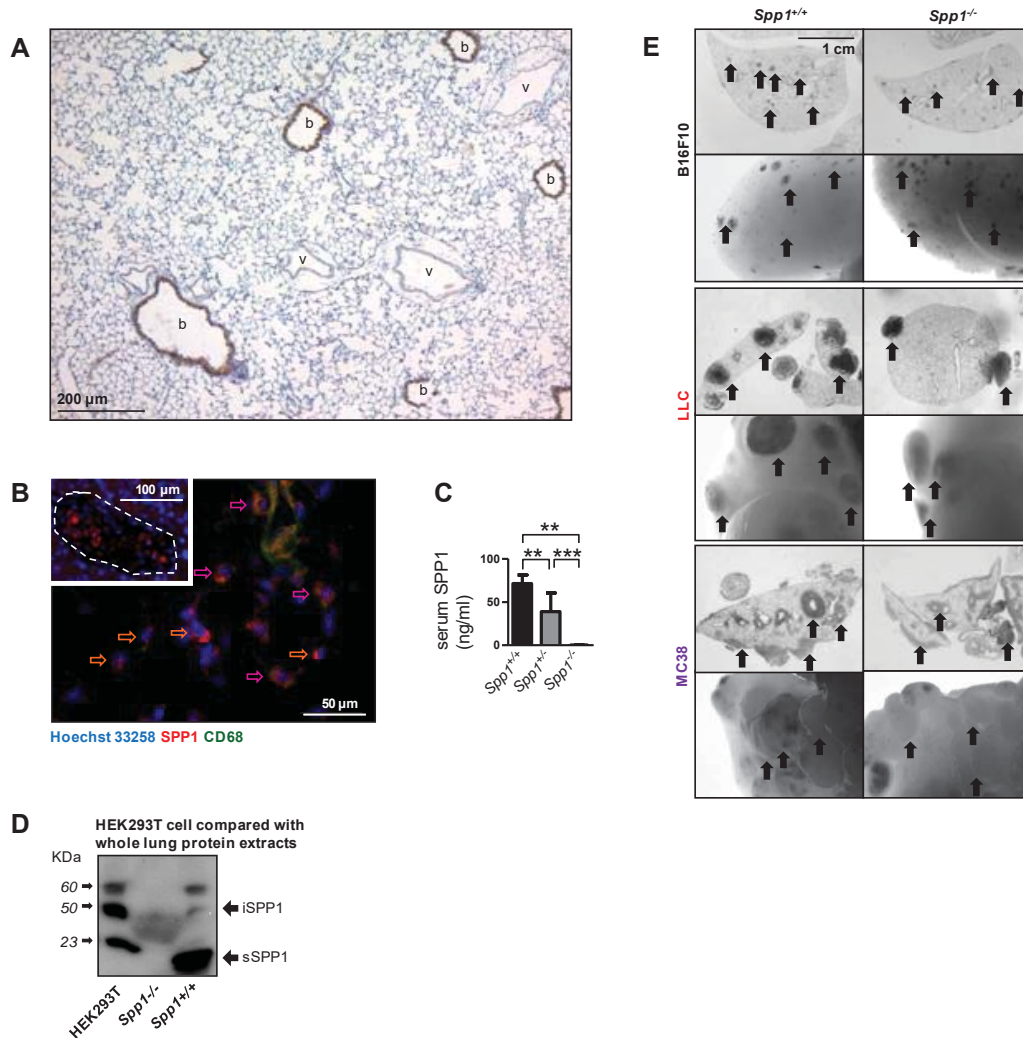


Figure S1 - SPP1 expression in the lungs and the bloodstream of mice. A. Representative image of immunostaining of the naïve *C57BL/6* mouse lung ($n = 5$) for endogenous SPP1 (brown), counterstained with hematoxylin (blue), showing strong immunoreactivity of bronchi (b), but not of vessels (v). B. Co-localization of SPP1 and CD68 in frozen lung tissue specimens. Type II alveolar cells express exclusively SPP1 (orange arrows) while macrophages both SPP1 and CD68 (pink arrows). Inlay: rib cartilage tissue (dashed outline) is shown as a positive control for SPP1 and a negative control for CD68. C. SPP1 protein levels in serum from the venous blood from *Spp1*^{+/+}, *Spp1*^{+/-} and *Spp1*^{-/-} mice by ELISA ($n = 6$ /group). Data are expressed as mean \pm SD. ** and ***: $P < 0.01$ and $P < 0.001$, respectively, for the indicated comparisons by one-way ANOVA with Bonferroni post-tests. D. Comparative immunoblot of whole lung protein extracts from *Spp1*^{+/+} and *Spp1*^{-/-} mice with extracts from HEK293T cells that express both intracellular (i) and secreted (s) SPP1 isoforms shows predominant sSPP1 expression in the lungs of *Spp1*^{+/+} mice and complete absence of SPP1 expression in the lungs of *Spp1*^{-/-} mice. E. Representative images from experiment in Figure 1D. Shown are microscopic images of lung sections stained with hematoxylin and eosin (top rows) and stereoscopic images of lungs (bottom rows) of *Spp1*^{+/+} and *Spp1*^{-/-} mice taken at day14 after the intravenous delivery of MC38, LLC or B16F10 cancer cells. Arrows point to metastases.

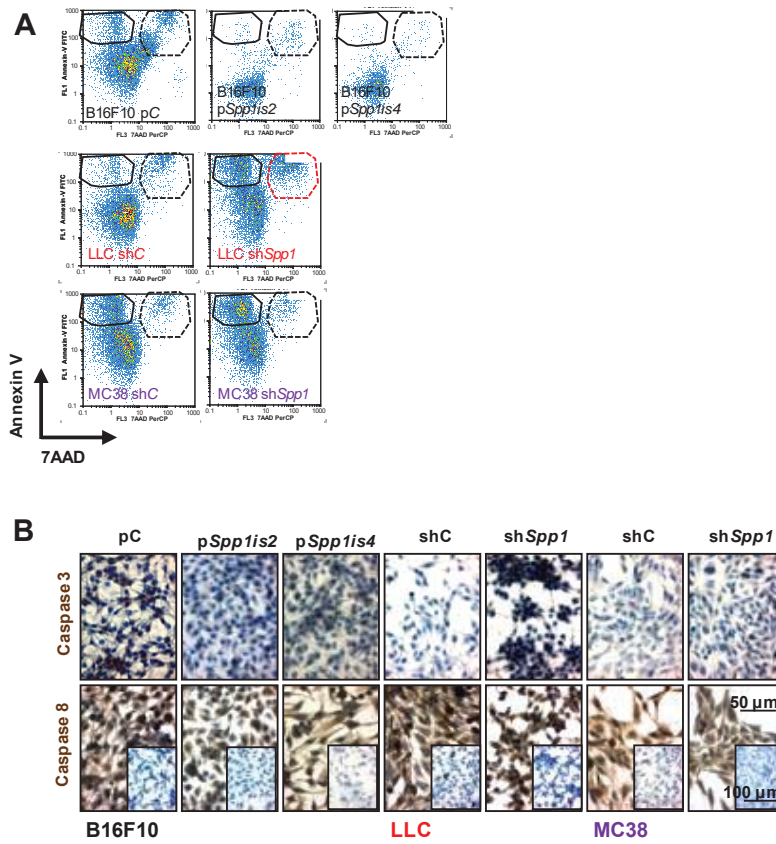


Figure S2 - SPP1 isoforms in tumor cell apoptosis. A. Representative dot-plots and gating strategy from the experiments described in Figure 2F. B. Representative immunocytochemistry images from the experiments described in Figure 2G. Inlays: isotype controls.

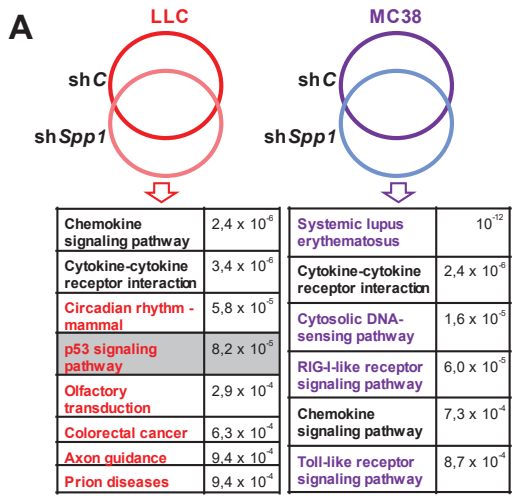
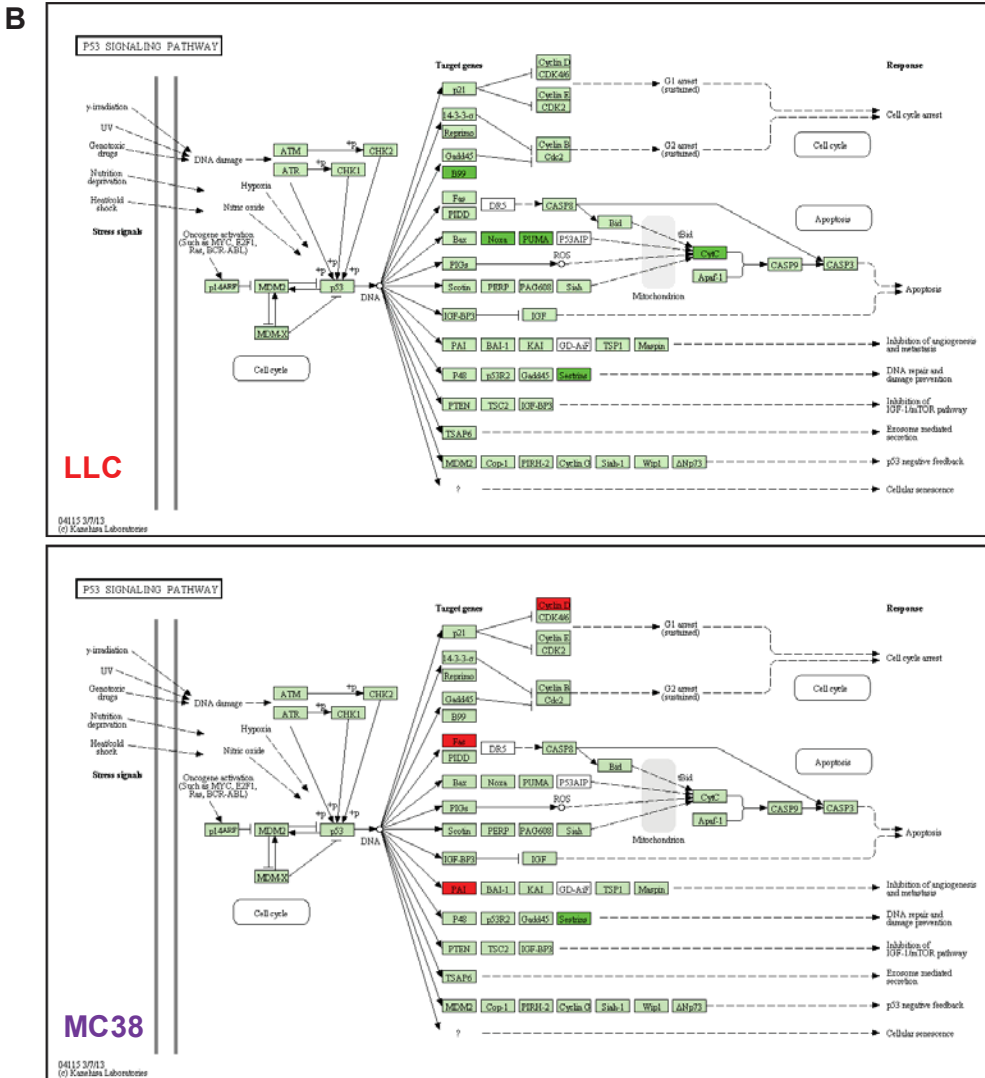


Figure S3 - Comparative pathway analysis of control- and *Spp1*-silenced LLC and MC38 cells. A. Transcripts represented differentially more than two-fold in control- and *Spp1*-silenced LLC and MC38 cells were entered into gene ontology (GO) pathway analysis. Shown are pathway names and probability values. Note commonly perturbed pathways in black font and unique pathways for each cell line in red (LLC) and purple (MC38) fonts. Note the highlighted significant change in the P53



signaling pathway (shaded cells) exclusively in LLC cells. B. Comparative P53 signaling pathway map analysis of control- and *Spp1*-silenced LLC and MC38 cells. Shown are P53 pathway maps for LLC cells (top) and MC38 cells (bottom). Genes highly significantly up-regulated by *Spp1* silencing are indicated in intense green color and genes highly significantly down-regulated by *Spp1* silencing in intense red color. Note that *Spp1* silencing in LLC cells strongly induced several P53 pathway components B99, Noxa, PUMA, CytC, and sestrins, while *Spp1* silencing in MC38 cells suppressed cyclin D, Fas, and PAI and induced only sestrins.

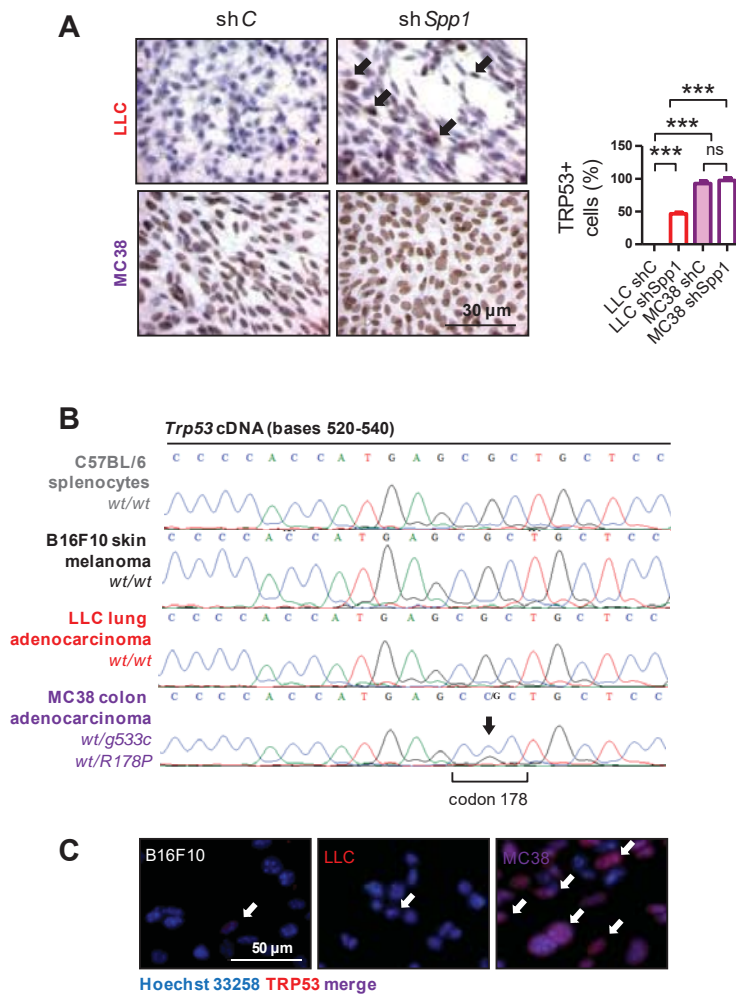


Figure S4 - A *Trp53* mutation in MC38 cells. A. Representative images (left) and data summary (right; $n = 5/\text{group}$) of TRP53 immunoreactivity (brown) of control- and *Spp1*-silenced LLC and MC38 cells, counterstained with hematoxylin (blue). Data are presented as mean \pm SD. ns and ***: $P > 0.05$ and $P < 0.001$, respectively, for the indicated comparisons by one-way ANOVA with Bonferroni post-tests. Note that *Spp1* silencing in LLC cells caused a statistically significant induction of nuclear TRP53 immunoreactivity (black arrows), which indicates increased stability or expression of TRP53 protein. In contrast, note the ubiquitous nuclear immunoreactivity of MC38 cells, which is not affected by silencing of *Spp1*, a pattern that suggests mutant TRP53. B. Sanger sequencing of *Trp53* cDNA obtained from total cellular RNA of murine splenocytes and from parental B16F10, LLC, and MC38 tumor cells. Note the heterozygous G to C miss-sense transversion in base 533, the second base of codon 178, of the *Trp53* transcript, which results in substitution of arginine (R) with proline (P). Note also the wild-type *Trp53* sequences of all other samples. C. Representative fluorescent images of TRP53 immunoreactivity (red) of B16F10, LLC, and MC38 tumor cells, counterstained with Hoechst 33258 (blue). Note the ubiquitous nuclear TRP53 immunoreactivity of MC38 cells versus the sporadic immunoreactivity of B16F10 and LLC cells (arrows), the former indicating mutant and the latter wild-type TRP53.

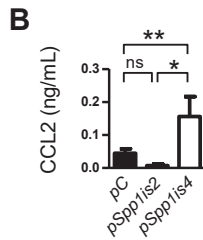
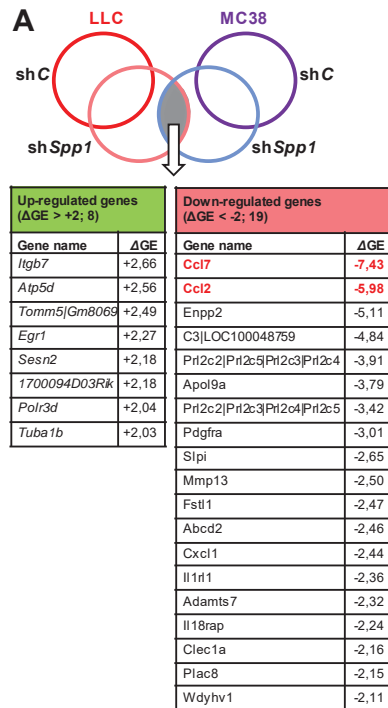


Figure S5 - CCL2 as a downstream partner of sSPP1. A. Comparative analysis of individual transcripts between control- and *Spp1*-silenced LLC and MC38 cells. Common transcripts represented differentially more than two-fold in control- and *Spp1*-silenced LLC and MC38 cells are shown. Shown are gene names and symbols, as well as mean changes in gene expression induced by *Spp1* silencing in LLC and MC38 cells combined. B. CCL2 protein levels by ELISA of culture media conditioned by B16F10 cells stably expressing constructs (p) encoding a random sequence (C), *Spp1is2*, or *Spp1is4*. Data are presented as mean \pm SD. ns, *, and **: $P > 0.05$, $P < 0.05$ and $P < 0.01$, respectively, for the indicated comparisons, by one-way ANOVA with Bonferroni post-tests.

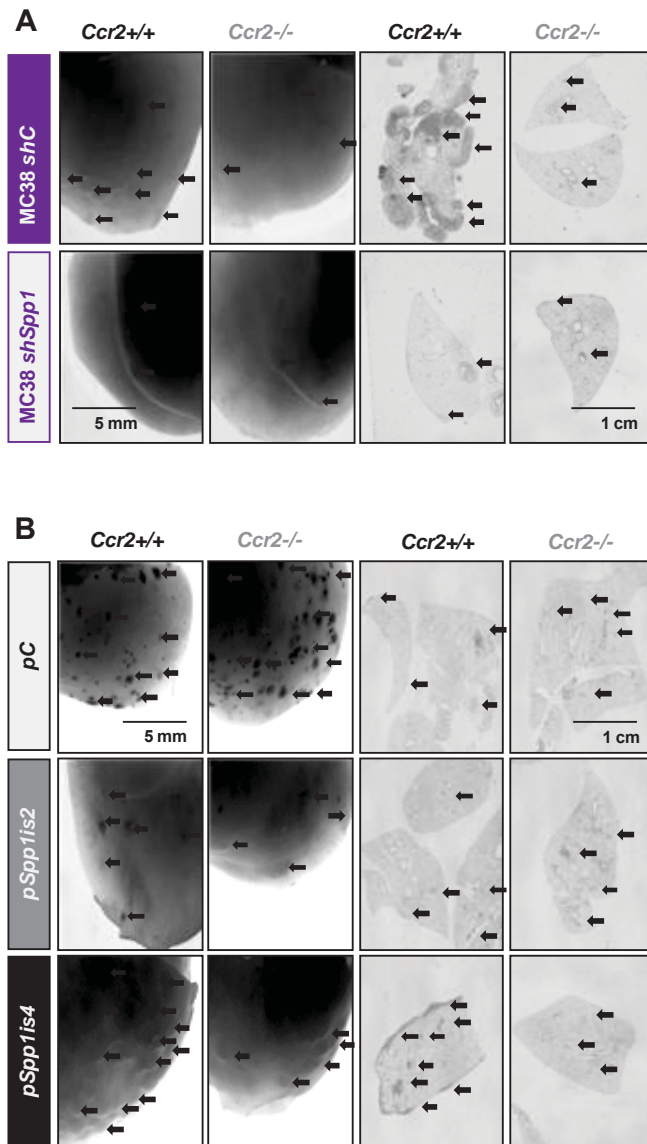


Figure S6 - Lung metastases induced in *Ccr2*-deficient mice by intravenous injection of parental and SPP1-modulated tumor cells. Representative stereoscopic (left) and microscopic (right) images of lung metastases (arrows) of *Ccr2*^{+/+} and *Ccr2*^{-/-} mice after i.v. injection of parental and SPP1-modulated MC38 (A) and B16F10 (B) cells described in Fig. 2.

SUPPLEMENTARY TABLES

Table S1 - Number of mice (*n*) used for these studies.

Figure number	Group	<i>n</i>
1C	Spp1+/+ mice with s.c. B16F10 cells	5
	Spp1-/- mice with s.c. B16F10 cells	6
	Spp1+/+ mice with s.c. LLC cells	7
	Spp1-/- mice with s.c. LLC cells	7
	Spp1+/+ mice with s.c. MC38 cells	7
	Spp1-/- mice with s.c. MC38 cells	7
1D	Spp1+/+ mice with i.v. B16F10 cells	6
	Spp1-/- mice with i.v. B16F10 cells	5
	Spp1+/+ mice with i.v. LLC cells	15
	Spp1-/- mice with i.v. LLC cells	12
	Spp1+/+ mice with i.v. MC38 cells	9
	Spp1-/- mice with i.v. MC38 cells	9
4A	<i>C57BL/6</i> mice with s.c. B16F10 pC cells	6
	<i>C57BL/6</i> mice with s.c. B16F10 p <i>Spp1is4</i> cells	6
4B	<i>C57BL/6</i> mice with s.c. MC38 shC cells	11
	<i>C57BL/6</i> mice with s.c. MC38 sh <i>Spp1</i> cells	11
4C-G	<i>C57BL/6</i> mice with s.c. LLC shC cells	14
	<i>C57BL/6</i> mice with s.c. LLC sh <i>Spp1</i> cells	16
5A	<i>C57BL/6</i> mice with i.v. B16F10 pC cells	5
	<i>C57BL/6</i> mice with i.v. B16F10 p <i>Spp1is2</i> cells	5
	<i>C57BL/6</i> mice with i.v. B16F10 p <i>Spp1is4</i> cells	5
	<i>C57BL/6</i> mice with i.v. LLC shC cells	20
	<i>C57BL/6</i> mice with i.v. LLC sh <i>Spp1</i> cells	24
	<i>C57BL/6</i> mice with i.v. MC38 shC cells	11
5B	<i>C57BL/6</i> mice with i.v. MC38 sh <i>Spp1</i> cells	11
	<i>C57BL/6</i> mice with i.v. LLC shC cells	9
	<i>C57BL/6</i> mice with i.v. LLC sh <i>Spp1</i> cells	7
	<i>C57BL/6</i> mice with i.v. MC38 shC cells	21
6D	<i>C57BL/6</i> mice with i.v. MC38 sh <i>Spp1</i> cells	13
	<i>Ccr2</i> +/+ mice with i.v. MC38 shC cells	9
	<i>Ccr2</i> -/- mice with i.v. MC38 sh <i>Spp1</i> cells	9
	<i>Ccr2</i> +/+ mice with i.v. MC38 shC cells	7
6E	<i>Ccr2</i> -/- mice with i.v. MC38 sh <i>Spp1</i> cells	8
	<i>Ccr2</i> +/+ mice with i.v. B16F10 pC cells	5
	<i>Ccr2</i> -/- mice with i.v. B16F10 pC cells	5
	<i>Ccr2</i> +/+ mice with i.v. B16F10 p <i>Spp1is2</i> cells	5
	<i>Ccr2</i> -/- mice with i.v. B16F10 p <i>Spp1is2</i> cells	4
	<i>Ccr2</i> +/+ mice with i.v. B16F10 p <i>Spp1is4</i> cells	5
	<i>Ccr2</i> -/- mice with i.v. B16F10 p <i>Spp1is4</i> cells	5
	Total	358

Table S2 - PCR primers used for these studies

Method ^a	Primer	Sequence
qPCR	mGusbF	TTACTTTAAGACGCTGATCACC
	mGusbR	ACCTCCAAATGCCCATAGTC
	mSpp1F	GATGAACAGTATCCTGATGCCAC
	mSpp1R	CCCTTTCCGTTGTTGTCCTG
	mCcl2F	AGGTCCTGTCATGCTTCTG
	mCcl2R	CGTAACTGCATCTGGCTGAG
	mCcl7F	CATCCACATGCTGCTATGTCA
	mCcl7R	CTTCCATGCCCTTCTTTGTCT
	mGapdhF	TGTGTCCGTCGTGGATCTGA
	mGapdhR	TTGCTGTTGAAGTCGCAGGAG
PCR	MycoplasmaSppF	GGGAGCAAACAGGATTAGATACCCT
	MycoplasmaSppR	TGCACCATCTGTCACTCTGTAAACCTC
RT-PCR	SPP1is2F	ATGAGGCTGCAGTTCTCCTGGC
	SPP1is4F	ATGAGATTGGCAGTGATTTGCTTTTG
	SPP1R	TTAGTTGACCTCAGAAGATGAACTCTC
	mTrp53F	GTAGCTTCAGTTCATTGGGA
	mTrp53R	GAAGTCATAAGACAGCAAGGA
CL	Spp1is2F	GCGCGCGGATCCATGAGGCTGCAGTTCTCCTG
	Spp1is4F	GCGCGCGGATCCATGAGATTGGCAGTGATTTGC
	Spp1is2/4R	GCGCGCGTCTGACTTAGTTGACCTCAGAAGATGA ACTC
	pBABEF	CCTTGAACCTCCTCTTTTCGAC
	pBABER	CTTTGCATACTTCTGCCTGCT

^a qPCR, quantitative (real-time) polymerase chain reaction; PCR, DNA polymerase chain reaction; RT -PCR, reverse transcriptase-polymerase chain reaction; CL, cloning.

Table S3 -Transcripts under-represented more than two-fold in both LLC and MC38 cells stably expressing anti-*Spp1*-specific shRNA compared with control LLC and MC38 cells stably expressing random sequence shRNA.

Gene Symbol	Gene Name	Fold-Change
<i>Ccl7</i>	chemokine (C-C motif) ligand 7	-7,43
<i>Ccl2</i>	chemokine (C-C motif) ligand 2	-5,98
<i>Enpp2</i>	ectonucleotide pyrophosphatase/phosphodiesterase 2	-5,11
<i>C3 LOC100048759</i>	complement component 3 complement C3-like	-4,84
<i>Prl2c2-c5</i>	prolactin family 2, subfamily c, members 2-5	-3,91
<i>Apol9a</i>	apolipoprotein L 9a	-3,79
<i>Pdgfra</i>	platelet derived growth factor receptor, alpha polypeptide	-3,01
<i>Sipi</i>	secretory leukocyte peptidase inhibitor	-2,65
<i>Mmp13</i>	matrix metalloproteinase 13	-2,50
<i>Fstl1</i>	follistatin-like 1	-2,47
<i>Abcd2</i>	ATP-binding cassette, sub-family D (ALD), member 2	-2,46
<i>Cxcl1</i>	chemokine (C-X-C motif) ligand 1	-2,44
<i>Il1rl1</i>	interleukin 1 receptor-like 1	-2,36
<i>Adamts7</i>	a disintegrin-like and metalloproteinase (reprolysin type) with thrombospondin type 1 motif, 7	-2,32
<i>Il18rap</i>	interleukin 18 receptor accessory protein	-2,24
<i>Clec1a</i>	C-type lectin domain family 1, member a	-2,16
<i>Plac8</i>	placenta-specific 8	-2,15
<i>Wdyhv1</i>	WDYHV motif containing 1	-2,11

Table S4 - Transcripts over-represented more than two-fold in both LLC and MC38 cells stably expressing anti-*Spp1*-specific shRNA compared with control LLC and MC38 cells stably expressing random sequence shRNA.

Gene Symbol	Gene Name	Fold-Change
<i>Itgb7</i>	integrin beta 7	2,66
<i>Atp5d</i>	ATP synthase, H ⁺ transporting, mitochondrial F1 complex, delta subunit	2,56
<i>Tomm5 Gm8069</i>	translocase of outer mitochondrial membrane 5 homolog (yeast) predicted pseudogene 8069	2,49
<i>Egr1</i>	early growth response 1	2,27
<i>Sesn2</i>	sestrin 2	2,18
<i>1700094D03Rik</i>	RIKEN cDNA 1700094D03 gene	2,18
<i>Polr3d</i>	polymerase (RNA) III (DNA directed) polypeptide D	2,04
<i>Tuba1b</i>	tubulin, alpha 1B	2,03

SUPPLEMENTARY MATERIALS AND METHODS

Mice

C57BL/6 (#000664), B6.129S6-*Spp1*^{tm1Blh/J} (#004936), B6.129P2-*Trp53*^{tm1Bm/J} (#008462), and B6.129S4-*Ccr2*^{tm1lc/J} (#004999) mice obtained from Jackson Laboratories (Bar Harbor, ME) were bred in the University of Patras Center for Animal Models of Disease. Experiments were approved *a priori* by the local Veterinary Administration of the Prefecture of Western Greece (approvals # 3741/16.11.2010, 60291/3035/19.03.2012, and 118018/578/30.04.2014), and were conducted according to Directive 2010/63/EU. Experimental mice and littermate controls were sex-, weight (20-25 g)-, and age (6-12 week)-matched (for *n* see Table S1).

Cells

LLC and B16F10 cells were from the National Cancer Institute Tumor Repository (Frederick, MD); MC38 cells were a gift from Dr. Barbara Fingleton (Vanderbilt University, Nashville, TN); and HEK293T cells were from the American Type Culture Collection (Manassas, VA). Cell lines were tested biannually for identity and stability by short tandem repeats, Sanger sequencing for driver mutations, and microarray.

Constructs

LLC cells stably transfected with random (non-sense; control) and anti-*Spp1* (sh*Spp1*)-targeted shRNA constructs are described elsewhere ¹. MC38 cells were stably transfected with the same constructs and protocol, using random (shC), anti-*Spp1* (sh*Spp1*) shRNA 64-mers, cloned into the *pSuper.retro.puro* backbone (Oligoengine). shRNA sequence was

AGCTTAAAAAGCTTATGGACTGAGGTCAATCTCTTGAATTGACCTCAGTCCA
TAAGCGGG and target sequences were shC: GATCAGGACAACAACGGAA; and
sh*Spp1*: GCTTATGGACTGAGGTCAA.

B16F10 cells and HEK293T human cells were stably or transiently transfected with pBabe (Addgene ID #1765) plasmids overexpressing SPP1: total RNA from murine MC38 cancer cells was isolated with the RNAeasy kit (Qiagen) according to the manufacturer's instructions. RNA was reverse-transcribed to *Spp1* cDNA by RT-PCR (see Table S2). *Spp1* cDNA was then amplified via PCR, using specific primers for two different products corresponding to isoform 2 and 4 respectively, which then were subcloned into pBabe vector (Addgene IDs #74411 and #74410, respectively) or pGFP-C1 (Takara Clontech Bio Company) with Addgene ID's #58247 and #58248 respectively. Cells were transfected with 5 µg DNA using Xfect™ Transfection Reagent (Takara Clontech Bio Company, # 631317) according to the manufacturers' instructions. Stable clones were generated by selection using hygromycin or G418.

Metastasis models

For spontaneous lung metastases, 100µl phosphate-buffered saline (PBS) containing either 10⁶ LLC, 10⁶ MC38, or 0.25 x 10⁶ B16F10 cells were injected s.c in mice thigh. For forced lung metastases, 100µl phosphate-buffered saline (PBS) containing either 0.25 x 10⁶ LLC, 0.25 x 10⁶ MC38, or 0.15 x 10⁶ B16F10 cells were injected into the tail vein ². Mice were sacrificed 30 days after s.c. or 14 days after i.v. for metastasis analyses, or when moribund for survival analyses. For spontaneous lung metastasis model three vertical tumor dimensions (δ1, δ2 and δ3) were monitored weekly.

Primary tumor volume was calculated using the formula: $\pi * \delta_1 * \delta_2 * \delta_3 / 6^3$. Lungs were fixed in 10% neutral buffered formalin overnight and the number of lung metastasis was evaluated by two blinded investigators (IG and GTS) and averaged. Lung volume was measured by saline immersion, and lungs were embedded in paraffin, randomly sampled by cutting 4 μ m-thick lung sections ($n = 10$ /lung), mounted on glass slides, and stained with H&E. Lung tumor burden was determined by point counting of the ratio of the area occupied by metastases versus the lung area and by extrapolating the average ratio per mouse to total lung volume⁴.

Primary mouse lung adenocarcinoma cells

Trp53^{fl/fl} mice (C57BL/6 strain), carrying loxP sites on either side of both *Trp53* alleles (*Trp53^{fl/fl}*) received ten weekly intraperitoneal injections of the pulmonary carcinogen urethane (1g/kg) starting at six weeks of age and were sacrificed ten months later. Lungs were harvested under sterile conditions, tumors ($n = 10$) were enucleated, minced, passed through a 100 μ m-strainer, and cultured separately in DMEM 10% FBS containing 100 mg/ml penicillin and streptomycin. One clone was established after four weeks and was passaged more than 100 times over two years to successfully yield one tumor cell line (CULA).

Histology, immunohistochemistry, immunofluorescence, immunocytochemistry

Whole lungs from sacrificed mice were fixed in 10% or 4% paraformaldehyde overnight and were embedded in paraffin or in OCT (Sakura). For immunohistochemistry, 4- μ m thick paraffin-embedded tissue sections were deparaffinized, rehydrated, and boiled in heat-induced epitope retrieval solution (10 mM sodium citrate; pH = 6.0). Endogenous peroxidase activity was inhibited using 3% H₂O₂ and non-specific antibody-protein binding was prevented using 3% bovine-serum albumin. Anti-SPP1 (ab8448, rabbit polyclonal IgG, in 1:100 dilution, Abcam) and anti-PCNA (ab2426, rabbit polyclonal IgG, 1:3000 dilution, Abcam) primary antibodies were used overnight at 4°C. Detection of primary antibody was performed with a horse radish peroxidase-conjugated polymer according to the manufacturer's instructions (EnVision; Dako, Glostrup). Sections were counterstained with Harris's hematoxylin, dehydrated, and mounted. Images were taken using an upright Axio Lab.A1 microscope connected to an AxioCam ERc 5s camera (Zeiss, Jena). For immunofluorescence, 10- μ m thick tissue sections were prepared as described above and incubated with anti-SPP1 (ab8448, rabbit polyclonal IgG; in 1:100 dilution, Abcam), rat anti-mouse CD68 (FA-11, purified IgG conjugated to Alexa fluo^R 488, 1:100 dilution, BioRad- Serotec) followed by nuclear counterstaining with Hoechst 33258 (Molecular Probes). Detection of primary antibody was performed using donkey anti-rabbit Alexa568-conjugated (A10042; 1/500 dilution; Invitrogen) secondary antibody. Immunoreactivity was captured on a Zeiss Axio Observer.D1 inverted microscope connected to an AxioCam MRc 5 camera (Zeiss, Jena) and was co-registered using Fiji academic imaging freeware (<http://fiji.sc/Fiji>). For immunocytochemistry, all cell lines were cultured on polylysine glass slides (10⁵ cells/well) and mounted with cold methanol. To prevent non specific antibody-protein binding slides were incubated in fetal bovine serum. The following primary antibodies and dilutions were used: anti-SPP1 (Abcam ab8448, rabbit polyclonal IgG; 1:100 dilution), anti-caspase 8 (Abcam ab25901, rabbit polyclonal IgG, 1:250 dilution), anti-caspase 3 (AF835, polyclonal rabbit IgG, 1:100 dilution, R&D systems) and anti-TRP53 antibody (Santa Cruz sc-6243, 1:250 dilution) for two hours. Detection of primary antibodies was performed as described above. For isotype controls, either or both primary antibodies were omitted and as positive control normal cartilage tissue was used.

Immunoblotting

Total protein extracts extracted by lysing 10^7 cultured were analyzed by using standard protocols. The following primary antibodies were used: anti-SPP1 (Abcam,; ab8448, rabbit polyclonal, 1:1000 dilution, and ab91655, rabbit monoclonal, 1:1000 dilution), anti-GFP (Santa Cruz; sc-9996, 1:500 dilution), anti-P53 (Santa Cruz; sc 6243, FL 393, 1: 200 dilution) and β -actin (Santa Cruz; sc 47788, mouse monoclonal IgG1, 1:500 dilution) followed by HRP-conjugated appropriate secondary antibodies (Southern Biotech; 4030-05, Goat anti-rabbit IgG, 1:8000 and Goat anti-mouse IgG, 1030-05, 1:8000 dilution).

Enzyme-linked immunosorbent assay (ELISA)

CCL2 and SPP1 protein levels of cell culture supernatants of 10^5 cells per well plated in six-well plates for 24 hours were determined using dedicated murine ELISA kits according to the manufacturer's instructions (Peprotech and R&D Systems).

Apoptosis assay

For the detection of early and late apoptotic cells, annexin-V-7AAD protocol was performed in samples of 10^6 cells. 100 μ l of cells in Annexin-V 1x buffer were incubated with Annexin-V PE (ImmunoTools; 31490014, 1:200 dilution) and 7AAD (eBioscience Inc; E00031-1632, 1:20 dilution), for 15 min in room temperature. Late apoptotic cells were characterized as Annexin-V⁺7AAD⁺, while early apoptotic cells as Annexin-V⁺7AAD⁻. All cancer cells were cultured and stained in triplicate. All results were analyzed on a CyFlow ML (Partec) and data were examined using FlowJo software (FlowJo).

Cellular assays

In vitro cancer cell proliferation of the various cell lines was determined using MTT reduction assay (Promega) in a concentration of 5mg/ml. All cell lines were cultured in triplicates in four 96-well plates in a total number of 3×10^3 cells per well. Each day of a total 4 days experiment, 10 μ L of 3-(4,5-dimethylthiazol-2-yl)-2,5-diphenyltetrazolium bromide working solution (5 mM MTT in PBS) was added to each well of a single plate. Four hours later, 100 μ L acidified isopropanol was added, followed by sediment solubilization. Absorbance was measured in a MR-96A microplate reader (Mindray) at 492 nm.

Quantitative Real-time PCR, Reverse transcriptase PCR, and microarray hybridization analysis

Total RNA from all cell lines was isolated using Trizol (ThermoFisher Scientific, 15596-026) followed by RNAeasy kit (Qiagen, 74104), and was reverse transcribed using Superscript III (Invitrogen, 18080044). *Gapdh* was used as control. qPCR was performed using first strand synthesis reactions along with the indicated primers and KAPA SYBR FAST qPCR Kit (Kapa Biosystems), in a StepOnePlus cycler (Applied Biosystems). The CT values from triplicate qPCR reactions were analyzed with the relative quantification method $2^{-\Delta\Delta CT}$ ⁵. The expression level of a given mRNA per sample/condition was determined relatively to reference gene mRNA levels. Reverse transcriptase-PCR primers are given in Table S2. For microarray, cells cultured in triplicate independent wells for each cell line-condition were subjected to RNA extraction as described above. Five μ g pooled RNA was tested for RNA quality on an ABI2000 bioanalyzer (Agilent Technologies), labeled, and hybridized to GeneChip Mouse Gene 1.0 or 2.0 ST arrays (Affymetrix). For analysis, the Affymetrix Expression Console (parameters: annotation confidence, full; summarization method:

iter-PLIER include DABG; background: PM-GCBG; normalization method: none) was used, followed by normalization of all arrays together using a Lowess multiarray algorithm. Intensity-dependent estimation of noise was used for statistical analysis of differential expression. Microarray data are available at the GEO database (<http://www.ncbi.nlm.nih.gov/geo/>; Accession ID: GSE79831).

Statistics

Sample size was calculated using power analysis on G*power academic freeware ⁶, assuming $\alpha = 0.05$, $\beta = 0.8$, and $\rho = 0.3$ (<http://www.gpower.hhu.de/>). No data were excluded from analysis. Data were collected by at least two blinded investigators from samples coded by a non-blinded investigator. All data were examined for normality of distribution by Kolmogorov-Smirnov test. Sample size (n) always refers to biological and not technical replicates. Data are expressed as mean \pm SD. Differences in means between two or multiple groups were examined by two-tailed Student's t-test or one-way ANOVA with Bonferoni post-tests, as appropriate, since data were distributed normally. Two-way ANOVA with Bonferoni post-tests was employed for analyses of cell and tumor growth. Survival proportions were examined by Kaplan-Meier analysis and log-rank test. All *P* values are two-tailed and were considered significant when < 0.05 . All statistics and plots were done using Prism v5.0 (GraphPad).

SUPPLEMENTARY REFERENCES

1. Psallidas I, Stathopoulos GT, Maniatis NA, Magkouta S, Moschos C, Karabela SP, et al. Secreted phosphoprotein-1 directly provokes vascular leakage to foster malignant pleural effusion. *Oncogene* 2013; 32:528-35.
2. Elkin M, Vlodaysky I. Tail vein assay of cancer metastasis. *Curr Protoc Cell Biol* 2001; Chapter 19:Unit 19 2.
3. Stathopoulos GT, Zhu Z, Everhart MB, Kalomenidis I, Lawson WE, Bilaceroglu S, et al. Nuclear factor-kappaB affects tumor progression in a mouse model of malignant pleural effusion. *Am J Respir Cell Mol Biol* 2006; 34:142-50.
4. Hsia CC, Hyde DM, Ochs M, Weibel ER. An official research policy statement of the American Thoracic Society/European Respiratory Society: standards for quantitative assessment of lung structure. *Am J Respir Crit Care Med* 2010; 181:394-418.
5. Pfaffl MW. A new mathematical model for relative quantification in real-time RT-PCR. *Nucleic Acids Res* 2001; 29:e45.
6. Faul F, Erdfelder E, Lang AG, Buchner A. G*Power 3: a flexible statistical power analysis program for the social, behavioral, and biomedical sciences. *Behav Res Methods* 2007; 39:175-91.